Forschungszentrum Karlsruhe
Technik und Umwelt

Wissenschaftliche Berichte
FZKA 5926

Development of a Tritium Permeation Barrier on MANET II Steel by Hot Dip Aluminising and Subsequent Heat Treatment

K. Stein-Fechner, H. Glasbrenner, J. Konys, O. Wedemeyer

Institut für Materialforschung
Projekt Kernfusion

Juni 1997

Forschungszentrum Karlsruhe
Technik und Umwelt
Wissenschaftliche Berichte
FZKA 5926

Development of a Tritium Permeation Barrier on MANET II Steel by Hot Dip Aluminising and Subsequent Heat Treatment

K. Stein-Fechner, H. Glasbrenner, J. Konys, O. Wedemeyer

Institut für Materialforschung

Projekt Kernfusion

Forschungszentrum Karlsruhe GmbH, Karlsruhe
1997

Forschungszentrum Karlsruhe GmbH
Postfach 3640, 76021 Karlsruhe

ISSN 0947-8620

Entwicklung von Tritiumpermeationshemmenden Schichten auf MANET II Stahl nach dem Hot-Dip Aluminierverfahren mit anschließender Wärmebehandlung

Zusammenfassung

In der vorliegenden Arbeit werden die Ergebnisse von MANET Blech- und Rohrproben diskutiert, die bei 700 °C, 30 s aluminiert wurden. Das Hot-Dip Aluminierverfahren ist sowohl für die Beschichtung von Blechen als auch für die Innen- und Außenbeschichtung von Rohren geeignet. Die gebildete $(Fe,Cr)_2Al_5$ Schicht hat bei Blechen eine Dicke von 15 - 20 µm, bei Rohren von 8 - 12 µm.

Die anschließende Wärmebehandlung von 950 °C, 2 h und 750 °C, 2 h bzw. 1075 °C, 0.5 h und 750 °C, 2 h, entspricht der Vergütungsvorschrift für MANET. Während der Wärmebehandlung wird die harte $(Fe,Cr)_2Al_5$ Schicht in zwei weniger spröde Phasen umgewandelt. Die dabei entstandene obere Schicht, (Fe,Cr)Al, ist ca. 20 - 30 µm dick, die untere, α-Fe(Cr,Al), ca. 70 - 110 µm. Die beiden Schichten sind durch ein Porenband voneinander getrennt.

Abstract

The present work describes the aluminising process on MANET sheets and pipes at 700 °C for 30 s. It will be shown that this method is well suitable for aluminising of sheets and pipes (∅ 10 mm) from the inside and outside as well. The thickness of the intermetallic scale $(Fe,Cr)_2Al_5$ formed on the sheet specimens is about 15 - 20 µm, on the pipe specimens about 8 - 12 µm.

The subsequent heat treatment was carried out at 950 °C, 2 h and 750 °C, 2 h or 1075 °C, 0.5 h and 750 °C, 2 h, resp. The heat treatments selected are the standard temperatures for reausteniting and subsequent tempering of MANET steel, which guarantee the original mechanical properties of the substrate material after the coating process. During the heat treatment, the hard and brittle $(Fe,Cr)_2Al_5$ scale is transformed into softer phases. The upper (Fe,Cr)Al phase is about 20 - 30 µm thick, the lower α-Fe (Cr, Al) phase about 70 - 110 µm. The two phases are separated by a band of high porosity.

Content

1. Introduction

In the fusion technology there is the need for tritium permeation barriers on low activation steels [1-3]. It is known that thin alumina scales can reduce the T-permeation rate by several orders of magnitude [4]. However, ceramic scales tend to fail already at very low deformations. Cracks within the alumina scale would indicate preferential paths for the T-permeation through the steel substrate. A suitable coating for technical application must therefore have the potential for rehealing of cracks. It seems that a coating of (Fe,Cr)Al phase or α-Fe(Cr,Al) solid solution should be able to fulfil this demand and also shows acceptable mechanical properties. Several methods have been developed to produce such scale systems on martensitic 8-10%Cr steels [5-9]. By hot dip aluminising for example, firstly a hard and brittle intermetallic $(Fe,Cr)_2Al_5$ scale is formed. A subsequent heat treatment transforms then this scale into desired softer phases and allows an alumina rich layer to form on top of the scale system.

2. Preparation of the Coating

2.1 Materials

The substrate material to be aluminised was the martensitic steel MANET II. The chemical composition of this steel is given in table 1.

C	Si	Mn	P	S	Cr	Ni	Mo	V	Nb	Fe
0.10	0.18	0.76	0.004	0.005	10.37	0.65	0.58	0.21	0.16	Bal.

Table 1: Chemical composition of MANET II (wt%).

The Al used for the Al melt had an initially purity of 99.5% with main impurities being Fe and Si. With increasing immersion time the melt became enriched in the main steel components Fe and Cr.

2.2 Sample Preparation

In order to demonstrate the usebility of the hot dipping process for both inside and outside coatings sample pipes and sheets have been investigated. The material was delivered in form of 4 mm thick sheet and 12 mm ∅ rod in tempered condition. Sample sheets were maschined by erosion. They had an extension of 50 mm x 15 mm x 1.5 mm. Sample pipes were maschined (∅=10 mm x 1 mm x 100 mm) by drilling a hole into a 12 mm ∅ rod. Each sample had a small hole on one side for hanging during the aluminising process.

After maschining the samples were sandblasted, degreased in acetone and finally cleaned ultrasonically in ethanol. As final surface preparation the cleaned specimens were dipped into flux solution (solution of KCl, NaCl and Na_3AlF_6 (ratio 5:4:1) in water) and dried.

2.3 Aluminising Process

Aluminising has been carried out by using the facility shown in figure 1. On its bottom a glove box is connected gas tight to a heated alumina crucible. As working atmosphere a reducing Ar-5%H_2 mixture was used since oxidation of the Al melt had to be avoided. The alumina crucible was filled with small Al pieces and heated up to 700°C by a furnace. The temperature was measured by a NiCr-Ni thermocouple which was protected by an alumina tube and placed directly in the Al melt. The samples, fixed by a hook and stainless steel wire to a crane system, were dipped into the melt. After 30 s of exposure they were pulled out of the melt. Cooling down took place in the glove box by natural cooling rate.

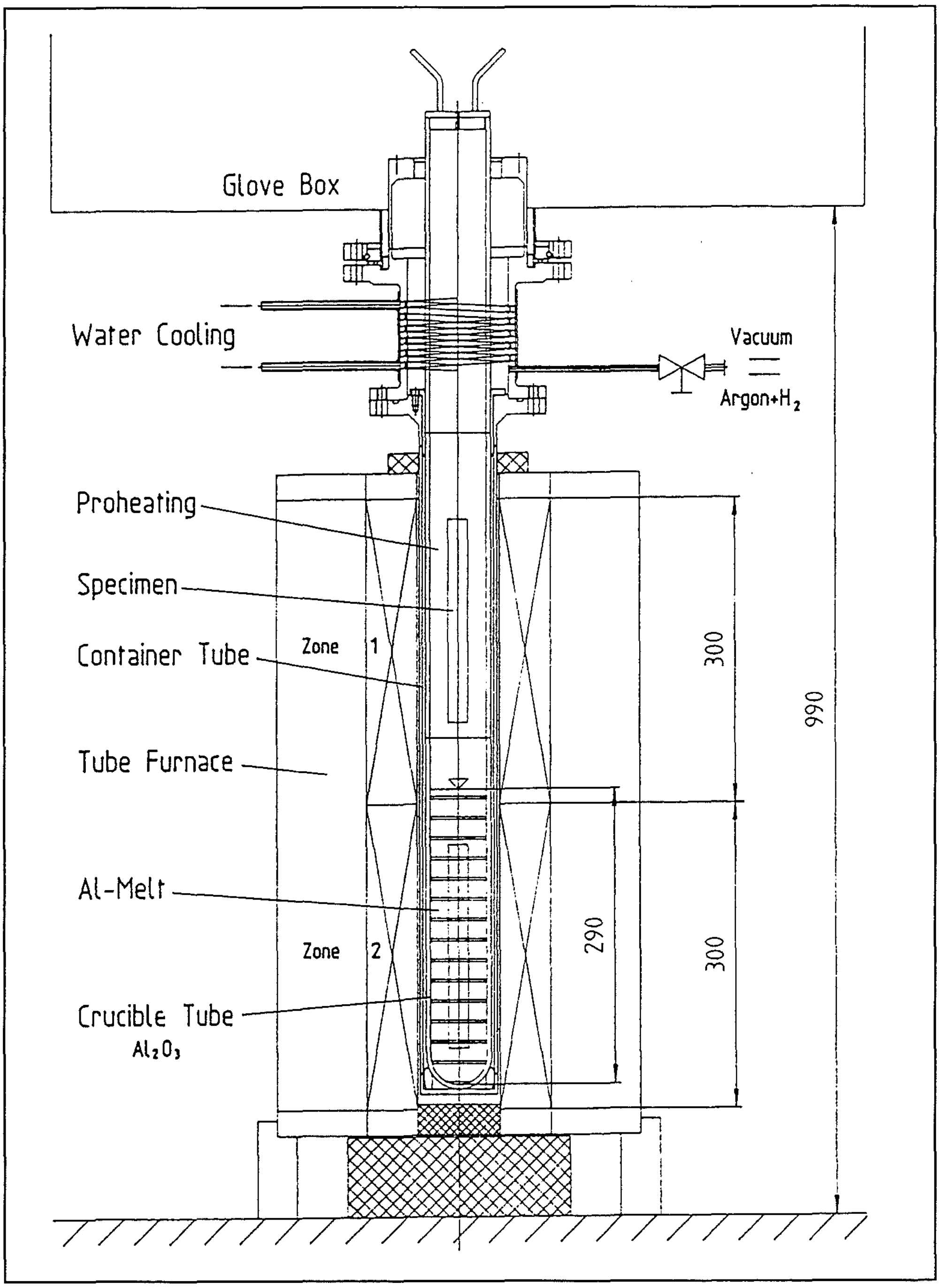

Figure 1: Aluminising facility

2.4 Heat Treatment

In order to optimise the coating structure in view of the demands of a tritium permeation barrier (TPB) a suitable heat treatment has to be carried out after aluminising. Goal of a successful heat treatment process must be:

-to incorporate completely the Al on the sample surface (solidified melt) into the steel matrix by diffusion

-to transform the brittle intermetallic scale, $(Fe,Cr)_2Al_5$, which formed during the aluminising process into a more ductile phase (preferable (Fe,Cr)Al or α-Fe(Cr,Al))

-to form a thin alumina-rich layer on top of the ductile aluminium enriched surface near scale as very efficient tritium permeation barrier with potential for self healing

-to guarantee the original mechanical properties of the substrate material after the coating process

-to keep the whole coating system as thin as possible since Al is an activating element and not desired in low activation steels

The heat treatment was carried out in a horizontal quartz rig. The aluminised samples were cleaned ultrasonically in ethanol, dried and placed in alumina crucibles which were positioned in the hot zone of the furnace. The working rig was flushed with Ar 6.0 and finally a flow rate of 5 l/h and a pressure of 1.25 bar were set. The heating rate was about 25 K/min. After the required holding time the crucibles were removed from the hot zone of the furnace and cooled down on air. The time and temperature regimes of the chosen heat treatments are listed in table 2.

type	**aluminising conditions T/t**	**heat treatment T/t**
A	700°C/30s	950°C/2h/air cooling 750°C/2h/air cooling
B	700°C/30s	1075°C/0.5h/air cooling 750°C/2h/air cooling

Table 2: Time and temperature regime of the heat treatment after aluminising

Extended investigations have shown that the fulfilment of the demands of TPB requires reaustening and subsequent tempering of the aluminised samples. Type A and B heat treatment, respectively were selected as alternative applications. Reaustening at 950°C instead of 1075°C results in smaller martensite grains. Up to now it is not yet clear whether smaller martensite grains and therefore very possibly a decrease of the creep properties will be accepted in view of the substrate properties.

3. Basic Characterisation of the Coating

3.1 Metallurgical and Chemical Characterisation

3.1.1 Aluminised Samples

Sheet specimens

After aluminising the samples were rather homogeneously covered by an about 60-70 μm thick overlayer of solidified Al melt as to be seen in figure 2a and b. Only on the bottom side of each sample a thicker overlayer of Al has been formed during the cooling phase since no tools were used to remove the melt drop. Beneath the Al overlayer an about 15-20 μm thick intermetallic scale has been formed mainly by Al diffusion into the steel substrate. The interface between the substrate and the intermetallic scale is smooth although the scale grew somewhat tongue like into the substrate, figure 2b. The interface between the Al overlayer and the intermetallic scale appears very inhomogeneous. This pattern is a good indication for two alternative processes: Crystal growth and desolution of the formed crystals and transport into the Al melt. Some cracks could be observed across the intermetallic scale. SEM/EDX point analyses have shown that the main part of the scale corresponds to $(Fe,Cr)_2Al_5$ phase. Just beneath the Al melt-intermetallic scale interface a higher Al concentration then for the rest of the scale was measured indicating the existence of the $(Fe,Cr)Al_3$ phase. Also, the striation like precipitates in the Al melt were found to be $(Fe,Cr)Al_3$ phase.

Pipe specimens

Pipe specimens have revealed a very similar scale structure and chemical composition compared to the sample sheets after aluminising. The inside and outside surfaces of the pipes were homogeneously covered by an about 2-8 μm thick overlayer of solidified Al melt. Beneath the Al overlayer an about 8-12 μm thick intermetallic scale has been formed. As an example the cross section of a pipe (inside wall) after aluminising is shown in figure 3a and b.

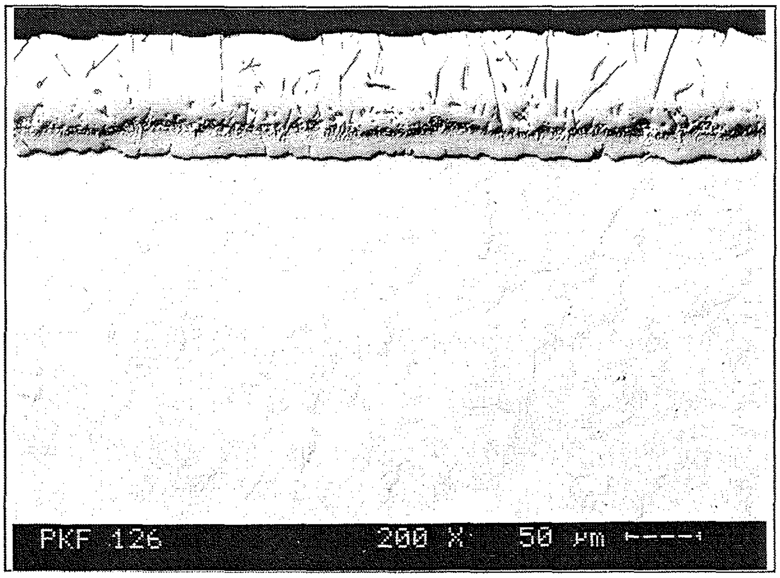

Figure 2a: Cross section of an aluminised MANET sheet (x 200)

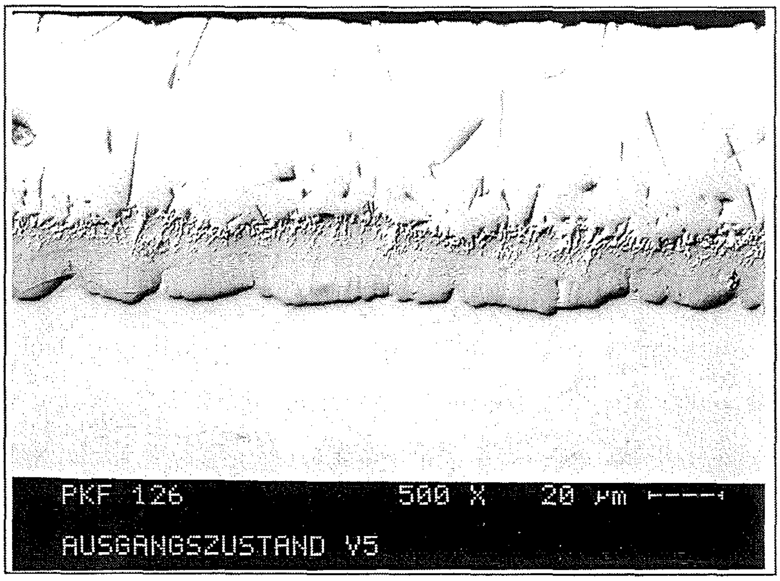

Figure 2b: Cross section of an aluminised MANET sheet (x 500)

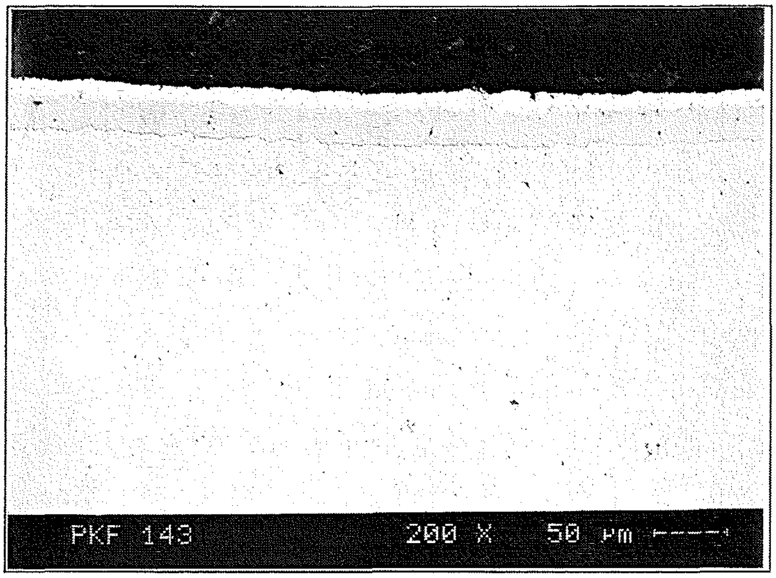

Figure 3a: Cross section of an aluminised MANET pipe (inside wall, x 200)

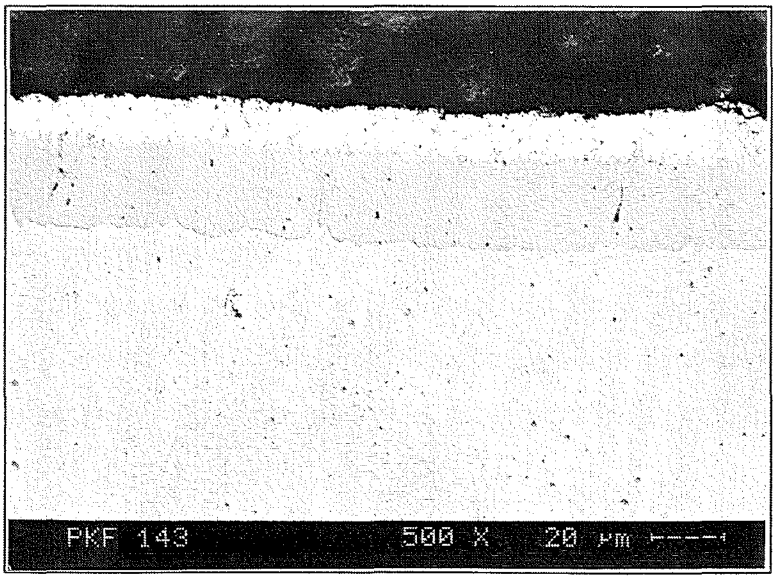

Figure 3b: Cross section of an aluminised MANET pipe (inside wall, x 500)

3.1.2 Samples after the Heat Treatment

Surface Investigation

Sheet specimens

SEM investigations have shown that the morphology of the sample surfaces appears similar for both types of heat treatment, A (950°C/2h, 750°C/2h) and B (1075°C/0.5h, 750°C/2h). The surface was homogeneously covered by an scale of small corrosion products as to be seen in figure 4a-f. On top of the scale indiviual crystalls have been formed which had a size between 20 and 60 µm. Amount and size of the indiviual corrosion products increased with higher temperature. EDX analyses revealed that the homogeneous surface scale mainly contains Al and smaller concentrations of Fe and Cr as shown in figure 5a. The indiviual corrosion products on top of this scale are composed of mainly Al and lower amounts of Cr and Fe, figure 5b. It can be seen that the individual crystalls are enriched in Cr compared to the scale. Oxygen could not been analysed by the used EDX system. However, it is very likely that the high Al concentration of the surface corrosion products indicates the presence of alumina rich compounds which contain some iron and chrominum oxides. Interesting to note that irregular oriented cracks were observed in the surface scale. For the heat treatment B (1075°C/0.5h, 750°C72h) more cracks were found then for the heat treatment A (950°C/2h, 750°C/2h). The crack flanks were overgrown by small corrosion products. Therefore it can be concludued that crack generation took place during quenching from the austinisation temperature (950 and 1075°C, respectively). During the subsequent tempering procedure at 750°C small corrosion products formed on the fresh crack surfaces.

Pipe specimens

The general morphology and chemical composition of the pipe surfaces were similar for both types of heat treatment, A and B and comparable to those of the sample sheets. The surface scale of sample pipes was cracked more frequently compared to the sample sheets. Also, the cracks appere sharper then on the flat surfaces. Small corrosion products can be seen on the crack flanks.

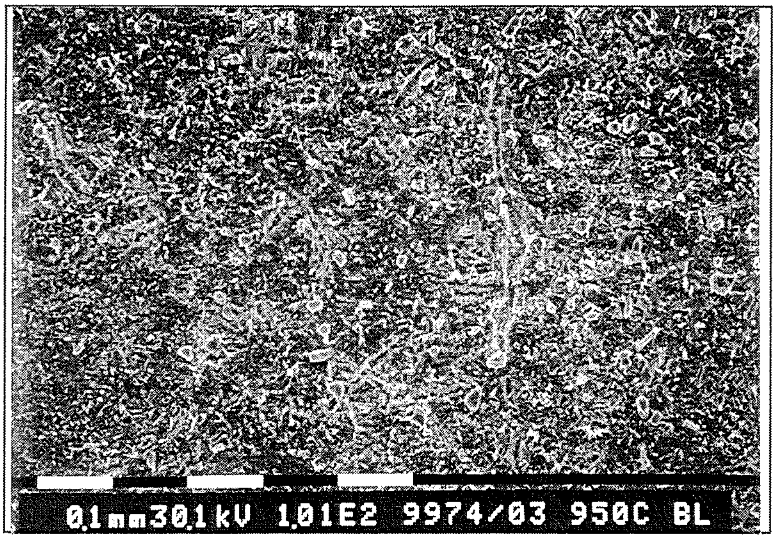

Figure 4a: Surface morphology of the heat treated sample sheet (type A: 950°C/2h, 750°C/2h, x 100)

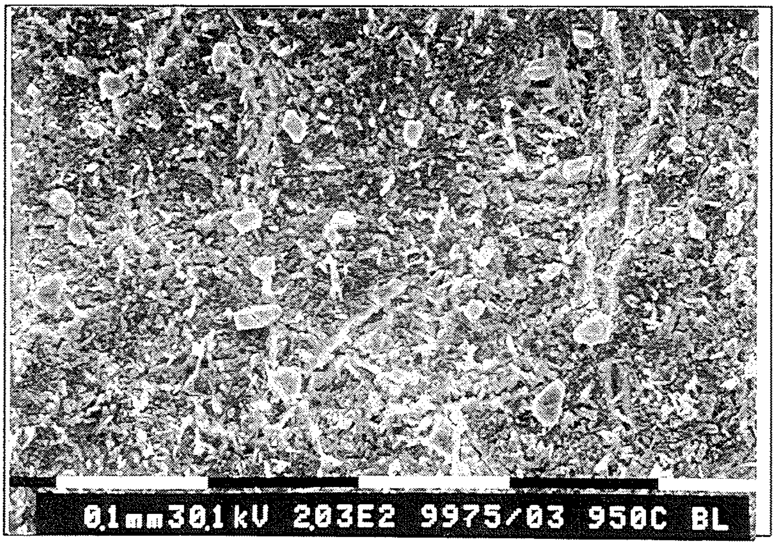

Figure 4b: Surface morphology of the heat treated sample sheet (type A: 950°C/2h, 750°C/2h, x 200)

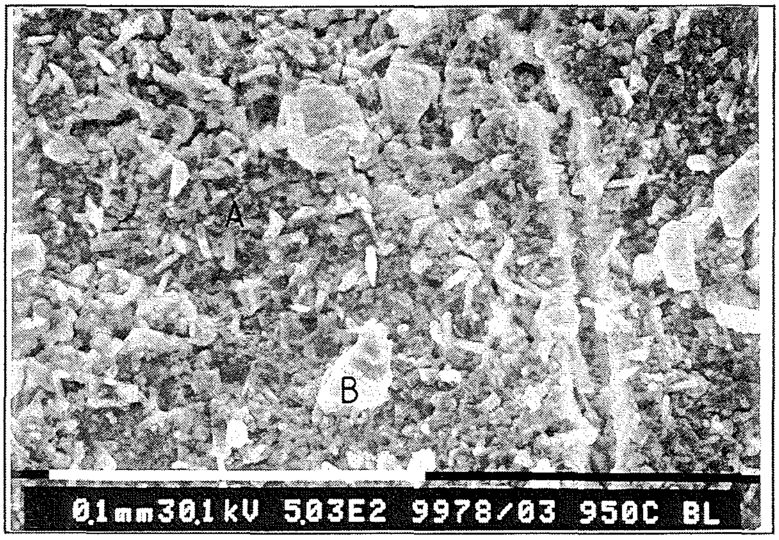

Figure 4c: Surface morphology of the heat treated sample sheet (type A: 950°C/2h, 750°C/2h, x 500)

Figure 4d: Surface morphology of the heat treated sample sheet (type B: 1075°C/0.5h, 750°C/2h, x 100)

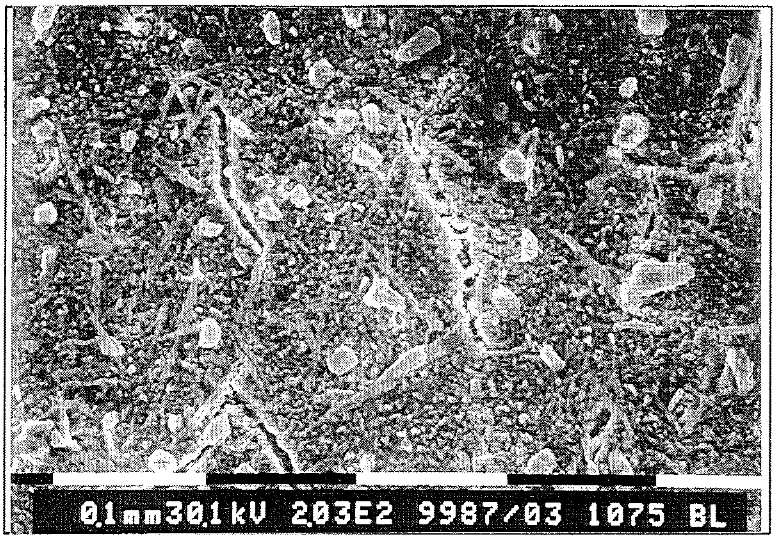

Figure 4e: Surface morphology of the heat treated sample sheet (type B: 1075°C/0.5h, 750°C/2h, x 200)

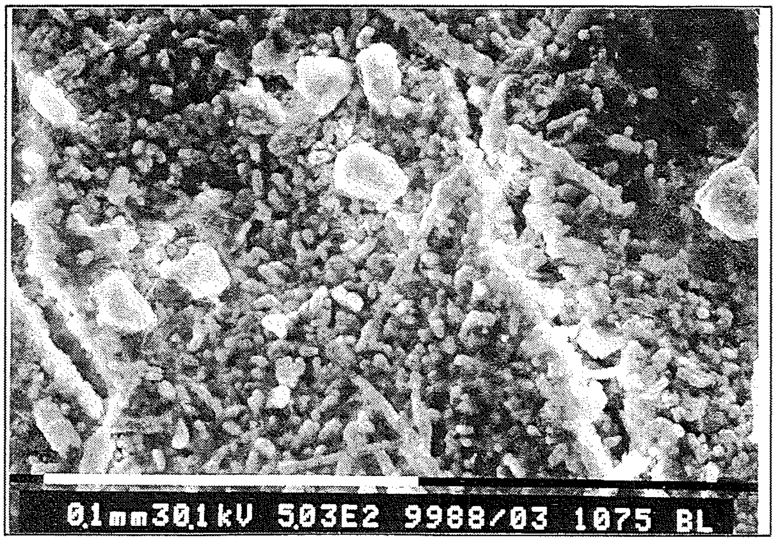

Figure 4f: Surface morphology of the heat treated sample sheet (type B: 1075°C/0.5h, 750°C/2h, x 500)

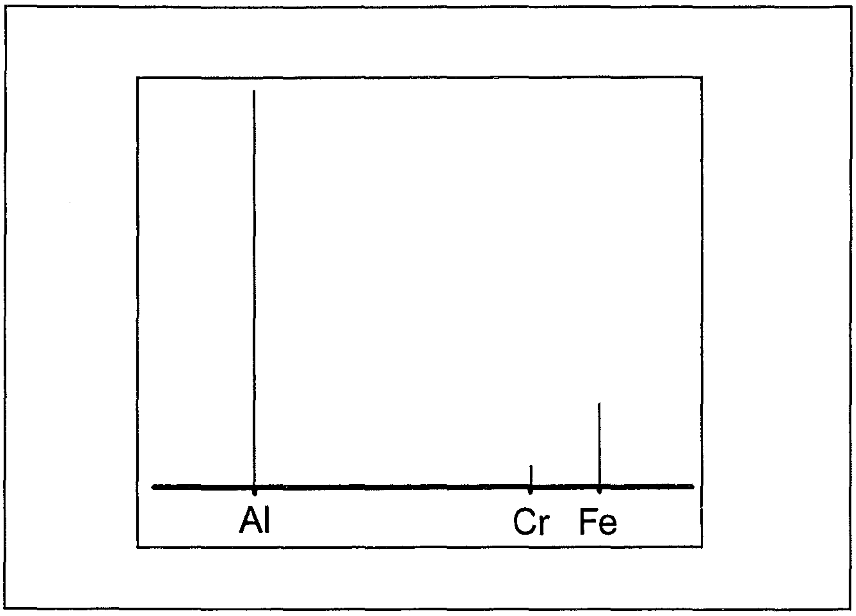

Figure 5a: EDX point analysis of the surface scale (position indicated by A in figure 4c)

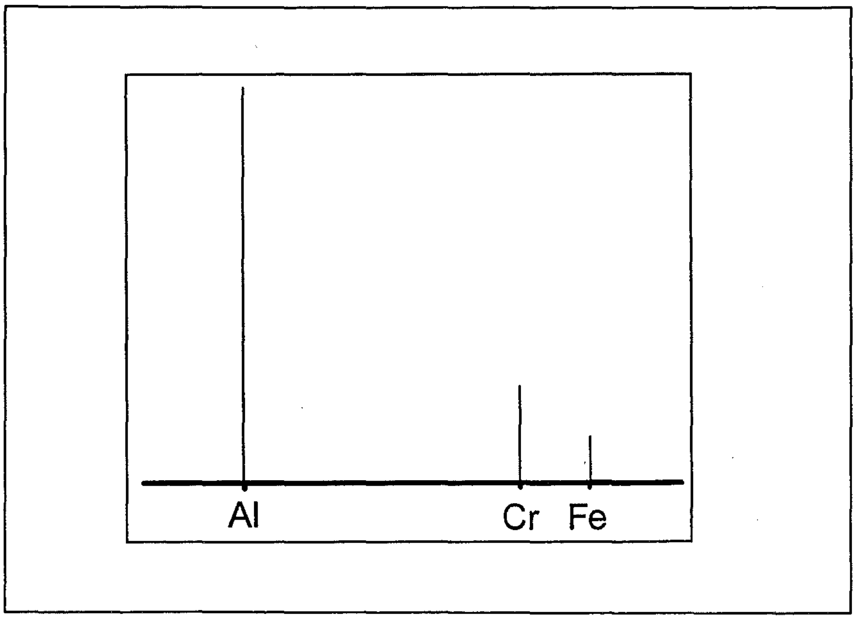

Figure 5b: EDX point analysis of the individual corrosion products on top of the surface scale (position indicated by B in figure 4c)

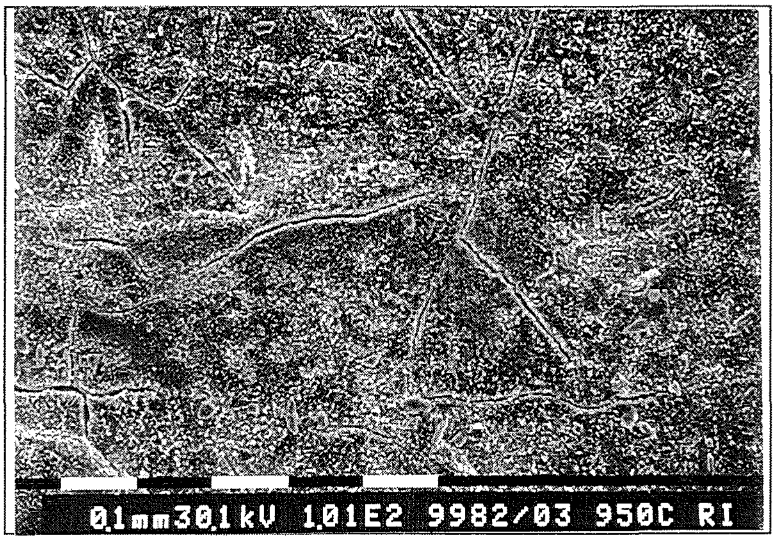

Figure 6a: Surface morphology of the heat treated sample pipe (type A: 950°C/2h, 750°C/2h, inside wall, x 100)

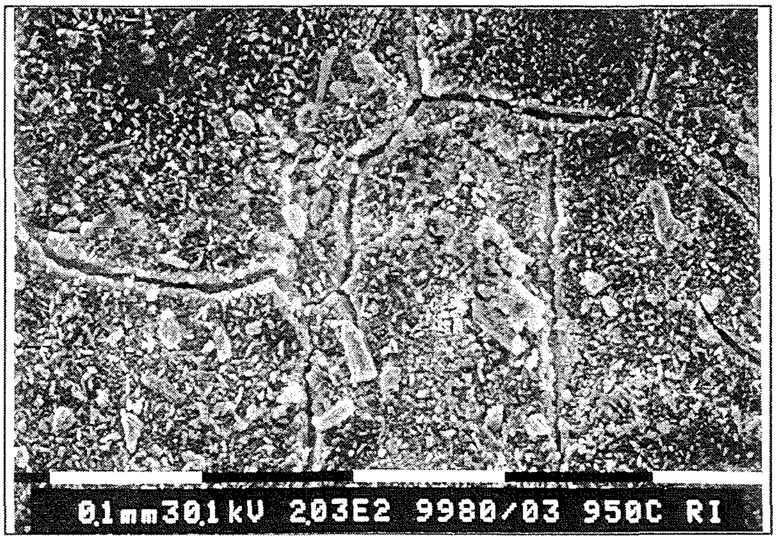

Figure 6b: Surface morphology of the heat treated sample pipe (type A: 950°C/2h, 750°C/2h, inside wall, x 200)

Figure 6c: Surface morphology of the heat treated sample pipe (type A: 950°C/2h, 750°C/2h, inside wall, x 500)

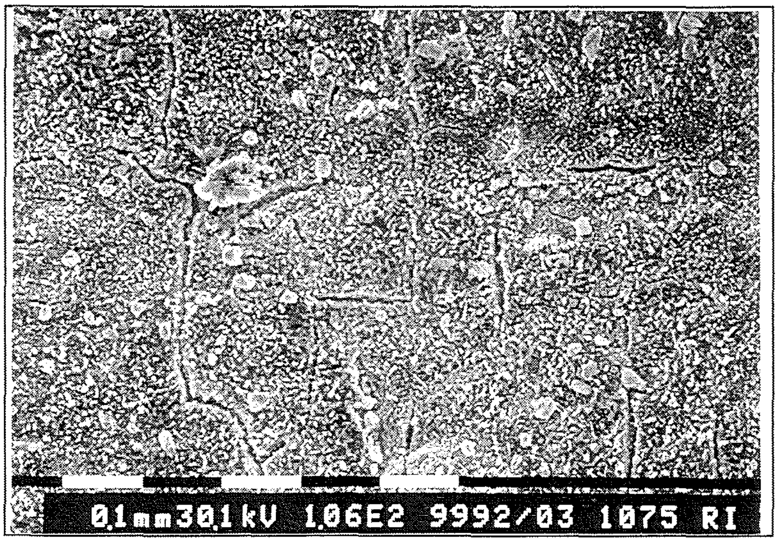

Figure 6d: Surface morphology of the heat treated sample pipe (type B: 1075°C/0.5h, 750°C/2h, inside wall, x 100)

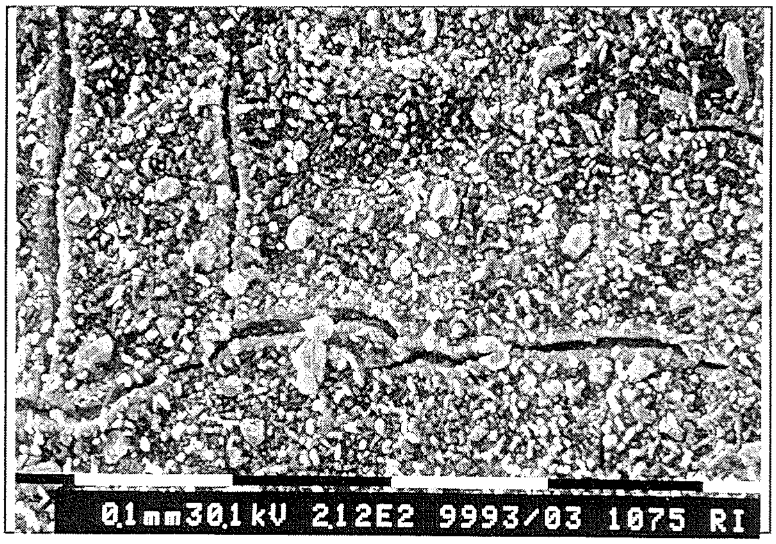

Figure 6e: Surface morphology of the heat treated sample pipe (type B: 1075°C/0.5h, 750°C/2h, inside wall, x 200)

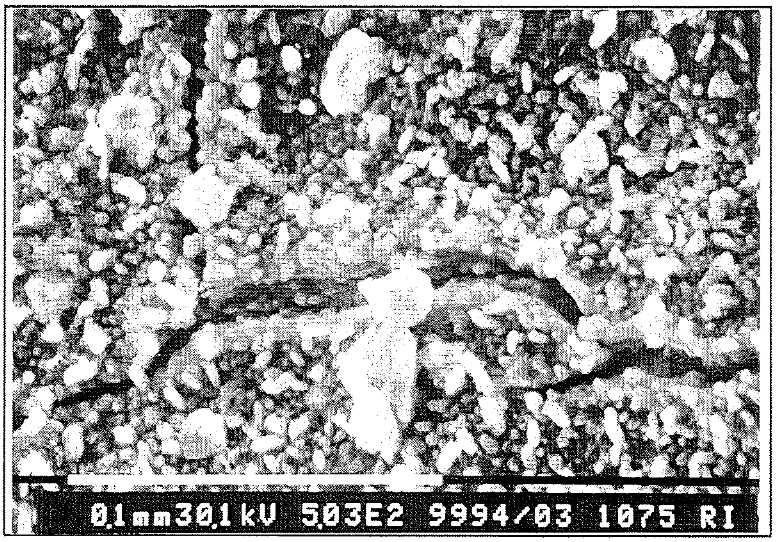

Figure 6f: Surface morphology of the heat treated sample pipe (type B: 1075°C/0.5h, 750°C/2h, inside wall, x 500)

Cross Sectional Investigation

Sheet specimens

The structure and chemical compsition of the scales were similar after both heat treatments, type A (950°C/2h, 750°C/2h) and B (1075°C/0.5h, 750°C/2h). The scale structure after heat treatment A and B is shown in figure 7a-c and 8a-c, respectively at various magnifications. The total scale thickness defined as the distance between the interface scale-substrate and the exterior surface of the coating was measured to be for type A and B samples about 100 and 150 µm, respectively. In general, the scale can be distinguished into an upper part of about 20-30 µm, an about 10-20 µm thick intermediate band of high porosity and a lower part of about 70-110 µm thickness. The interface to the substrate beneath is indicated as a sharp boundary. The sample surface is rather inhomogeneous. In the upper part of the scale, near to the surface, a few pores have formed but no cracks could be observed across the scale. The structure of the scale is characterised by large grains of up to 100 µm in width oriented perpendicular to the surface. In the lower part of the scale fine precipitations can be observed which are homogeneousely distributed. The grain structure beneath the scale has the typical appearance of a martensitic substrate. The EPMA line scan analysis of a sample which was heat treated under condition B (1075°C/0.5h, 750°C/2h) is shown in figure 9. It can be seen that the intermetallic $(Fe,Cr)_2Al_5$ phase has completely transformed after the heat treatment at 1075°C. There is a solely Al concentration on the surface indicating the existance of an alumina rich layer on top (oxygen has not been analysed). Just beneath the surface a region of the existance of (Fe,Cr)Al phase can be recognised. According to the binary Fe-Al phase diagram this phase is stable between 30-54 at% Al at 1075°C. The thickness of this zone which corresponds to the upper part of the scale is about 40 µm. The strong scatter of the concentration gradients beneath the (Fe,Cr)Al phase, indicated by "B" in figure 9, results from interactions of the electron beam with pores of the intermediate layer of the scale. A correct quantitative analysis is not possible there. For the lower part of the scale the Al concentration decreases more rapid then for the upper part. Within 110 µm the Al concentration decreases from 30 to 0 at%. For samples which were heat treated under condition A no line scan analysis was carried out, However, it can be expected that the elemental distribution across the scale is comparable to that for samples which were heat treated under condition B. Due to the slower diffusion rate at 950°C compared to the diffusion rate at 1075°C the extend of the individual zones of the scale might be smaller.

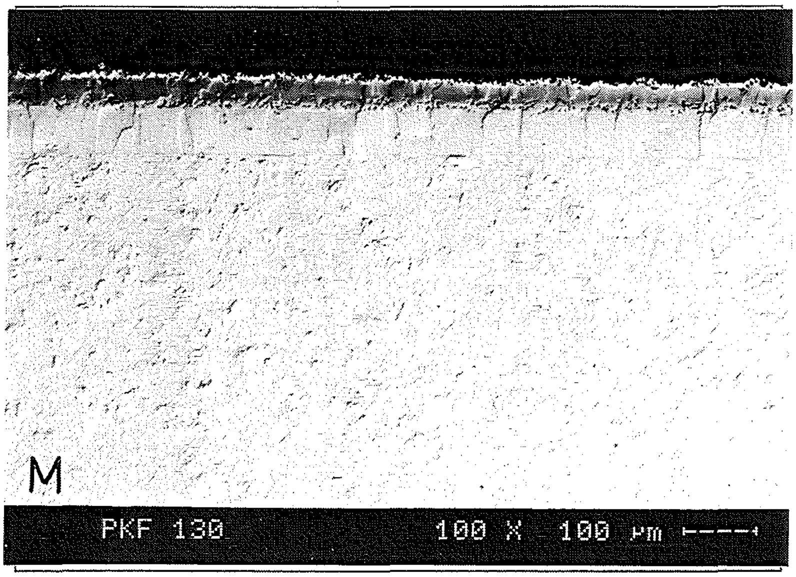

Figure 7a: Cross section of the heat treated sample sheet (type A: 950°C/2h, 750°C/2h, x 100)

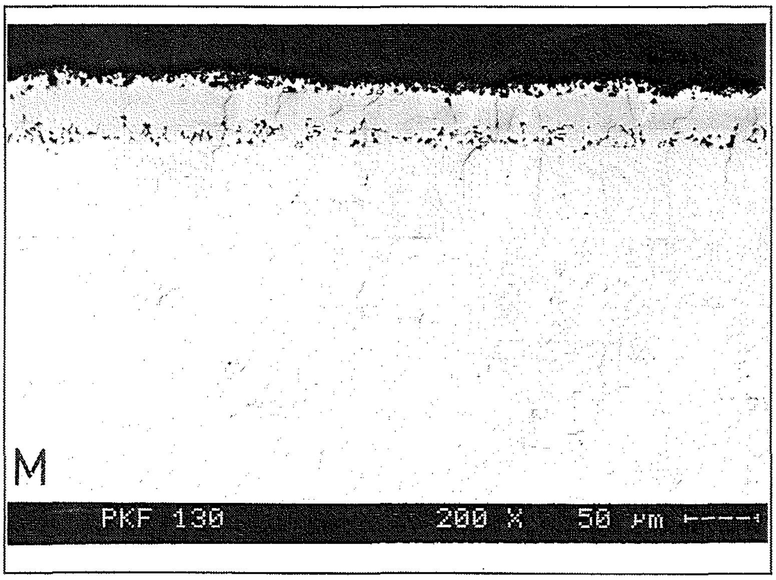

Figure 7b: Cross section of the heat treated sample sheet (type A: 950°C/2h, 750°C/2h, x 200)

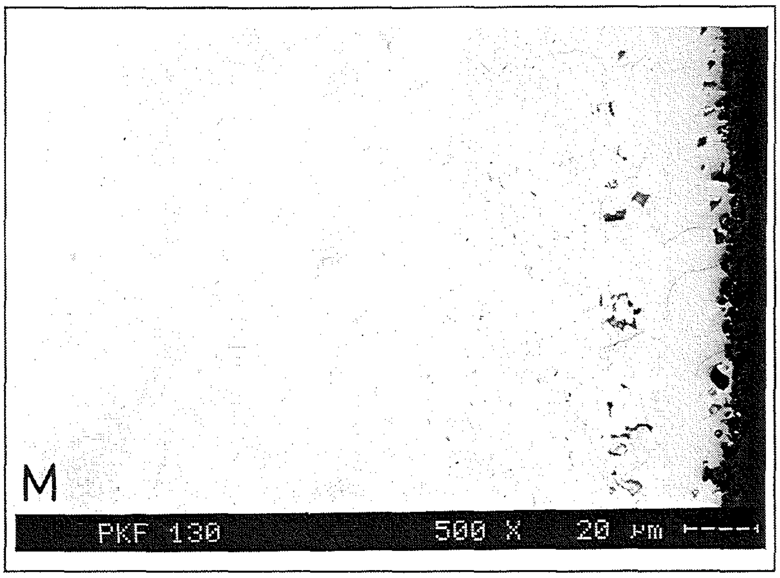

Figure 7c: Cross section of the heat treated sample sheet (type A: 950°C/2h, 750°C/2h, x 500)

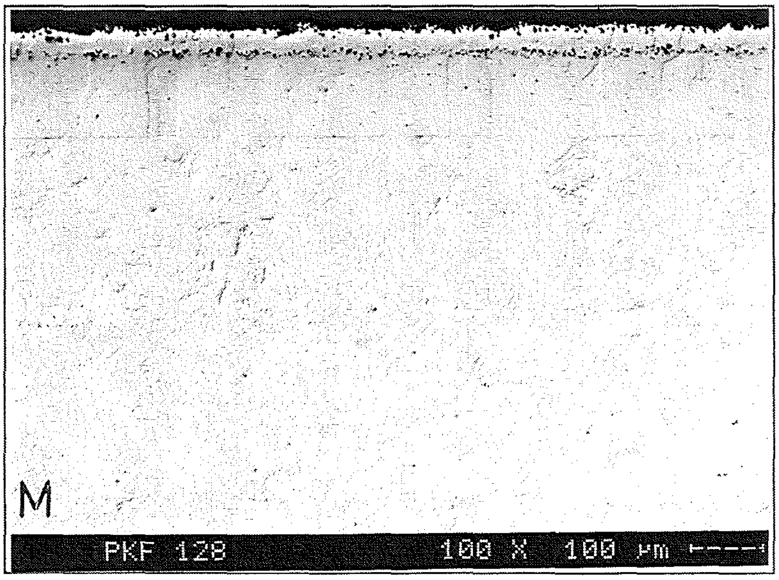

Figure 8a: Cross section of the heat treated sample sheet (type B: 1075°C/0.5h, 750°C/2h, x 100)

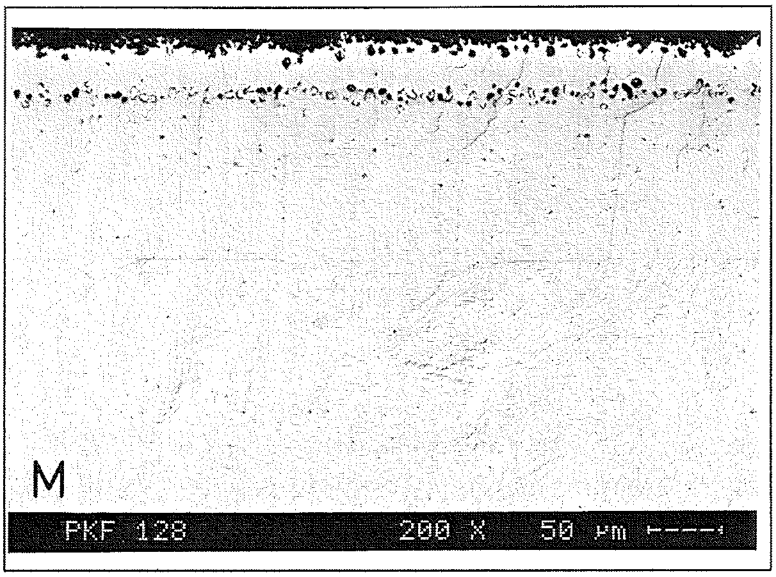

Figure 8b: Cross section of the heat treated sample sheet (type B: 1075°C/0.5h, 750°C/2h, x 200)

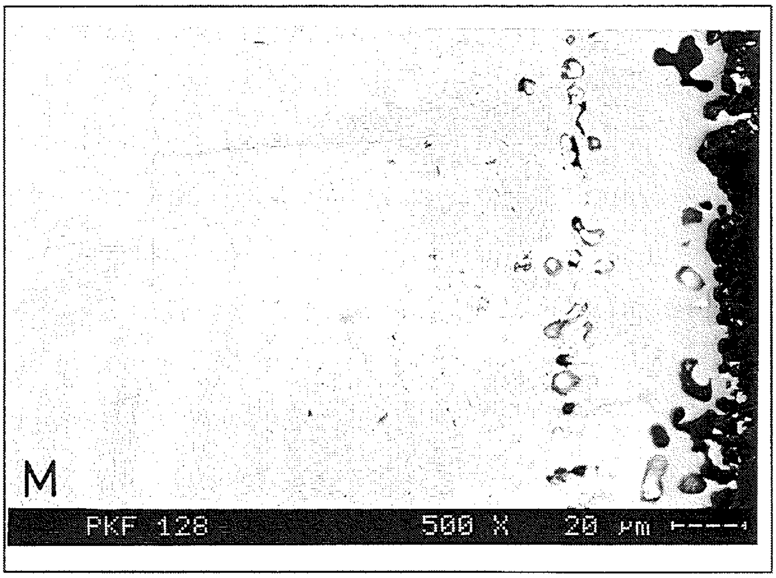

Figure 8c: Cross section of the heat treated sample sheet (type B: 1075°C/0.5h, 750°C/2h, x 500)

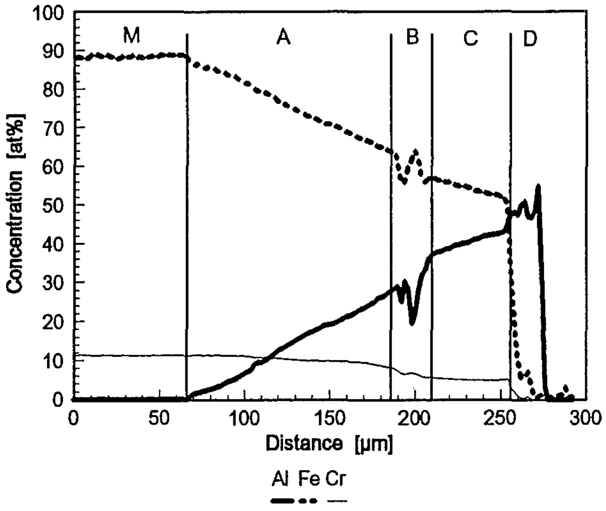

Figure 9: EPMA line scan of a heat treated sample sheet (type B: 1075°C/0.5h, 750°C/2h). M...matrix, A...α-Fe(Cr,Al), B...band of pores, C... (Fe,Cr)Al, D...surface scale

Pipe specimens

The structure and chemical compsition of the scales were similar after both heat treatments, type A (950°C/2h, 750°C/2h) and B (1075°C/0.5h, 750°C/2h). The scale structure after heat treatments A and B is shown in figure 10a,b and 11a,b, respectively for the outside and inside wall of the pipe specimens. No changes of the scale structures can be observed compared to the scale structures of the sheet specimens. The total scale thickness defined as the distance between the interface scale-substrate and the exterior surface of the coating was measured to be for type A and B samples about 100 and 125 µm, respectively. On all heat treated pipe specimens cracks could be observed across inside and outside coatings which generated at the surfaces and propagated through the upper part of the scale, as to be seen for instance in figure 10b for an inside wall. Sometimes those cracks were stoped already in the upper part of the scale but often they ended up within the band of pores. Crack propagation through the lower part of the scale was never observed. Such a crack pattern was never found on sheet specimens.

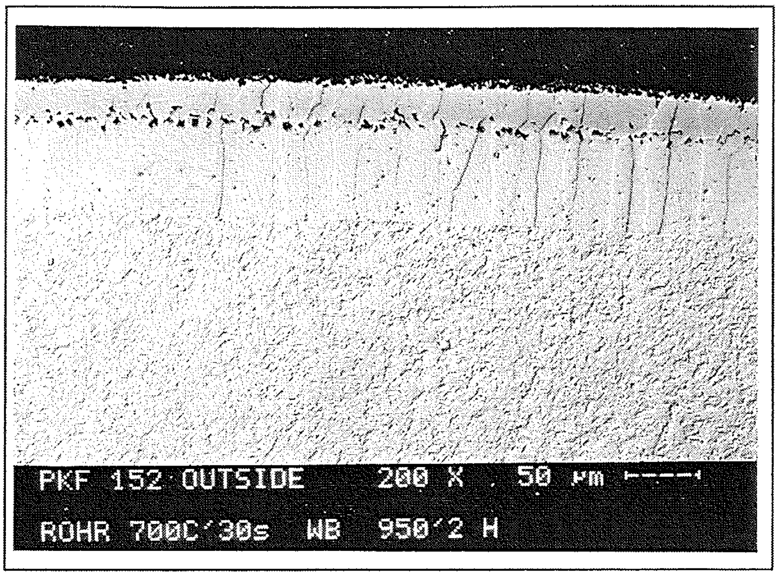

Figure 10a: Cross section of the heat treated sample pipe (type A: 950°C/2h, 750°C/2h, outside wall, x 200)

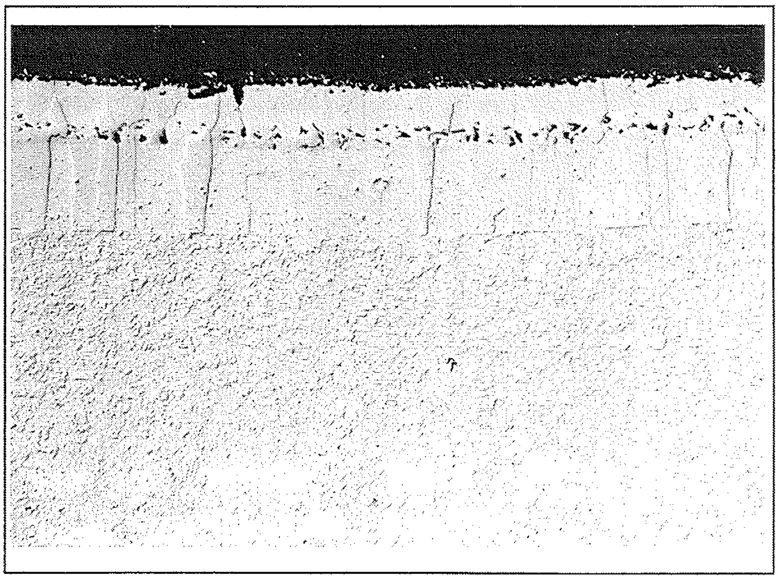

Figure 10b: Cross section of the heat treated sample pipe (type A: 950°C/2h, 750°C/2h, inside wall, x 200)

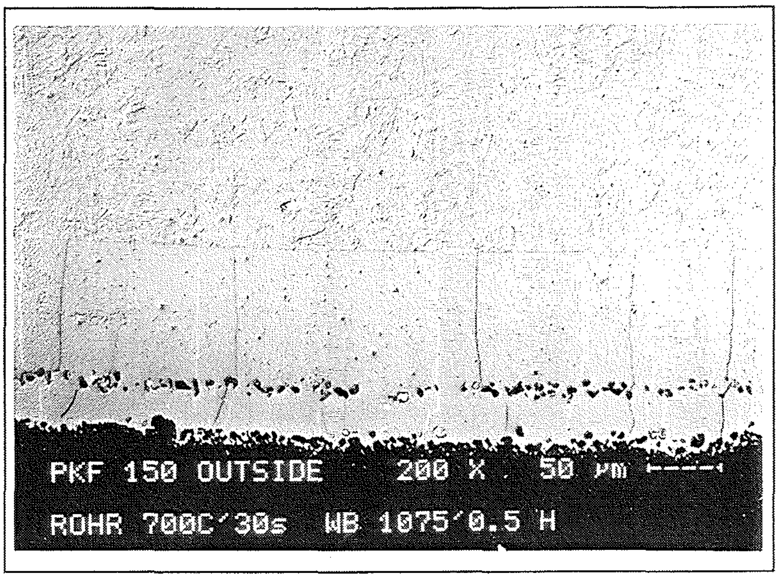

Figure 11a: Cross section of the heat treated sample pipe (type B: 1075°C/0.5h, 750°C/2h, outside wall, x 200)

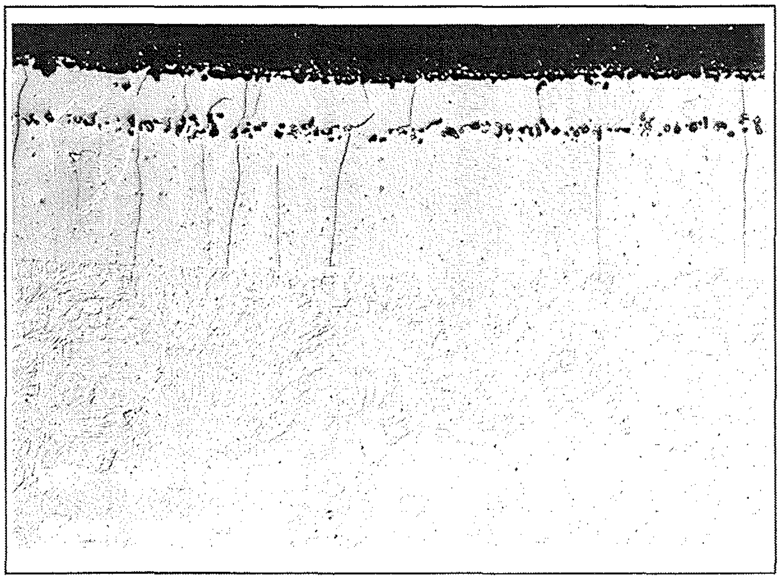

Figure 11b: Cross section of the heat treated sample pipe (type B: 1075°C/0.5h, 750°C/2h, inside wall, x 200)

Porosity

The determination of the porosity has been carried out by means of an image analyser. The cross sectional sample cuts have shown that the porosity of the coating varies very much. Pores can frequently be found in the upper part of the coating, just beneath the sample surface. Those pores are difficult to quantify since parts of the upper part of the scale tend to spall off. In the lowest part of the coating, the α-Fe(Cr,Al) zone, no pores were observed. For those reasons it seemed to be more relevant to determine the porosity of the intermediate band of high porosity separately and to compare both heat treatment types (A and B).

The image analyses were carried out on polished sample cuts at a magnification of x 400. The samples were measured at 5 different positions and an average value was calculated. In order to keep the area to be analysed constant for all samples a window of 60 µm x 15 µm was defined. The results of the porosity analysis are shown in table 3.

	A (950°C/2h, 750°C/2h)	**B (1075°C/0.5h, 750°C/2h)**
total porosity of the intermediate band of pores (15 µm thick)	7.1% ±1.9%	16.4% ±3.8%
average area of one pore	2.3 μm^2 ±1.0 μm^2	4.4 μm^2 ±0.5 μm^2

Table 3: Results of the porosity analysis

The investigations have shown that there is no difference in the results for sheet and pipe specimens. However, it is obvious that both values the total porosity and the average area of one pore increase with temperature.

3.2 Mechanical Characterisation

3.2.1 Vickers Microhardness (HV 0.05)

The hardness of the formed intermetallic scale after the aluminising process was about 1000-1100 HV 0.05. The hardness of the substrate remained unchanged compared to the virgin material. Results of the hardness measurements after the heat treatment are presented in table 4.

	HV 0.05 **A (950°C/2h, 750°C/2h)**	**HV 0.05** **B (1075°C/0.5h, 750°C/2h)**
upper part of the coating (Fe,Cr)Al	275 - 340	270-315
lower part of the coating α-Fe(Cr,Al)	325 (beneath band of pores) 240 215 (interface coating/steel)	335 (beneath band of pores) 290 200 (interface coating/steel)
substrate MANET II	220-250	235-270

Table 4: Results of microhardness measurement (HV 0.05)

4. Conclusions

The investigations have shown that Hot Dip Aluminising is a suitable method to introduce Al by a controlled manner into the surface near zone of MANET II steel. For both sample geometries, flat sheets and pipes, a very brittle intermetallic scale formed mainly by inward diffusion of Al into the steel during the immersion process. On top of this intermetallic scale an overlayer of solidified Al melt exists.

In order to meet the demands of a Tritium permeation barrier the aluminised specimen had to undergo a heat treatment at temperature above the A_{c1} temperature of the MANET II steel. It was found that both chosen heat treatments A (950°C/2h, 750°C/2h) and B (1075°C/0.5h, 750°C/2h) resulted in a very similar scale structure. The formed scale can be subdivided into three different zones after heat treatment: an upper layer of (Fe,Cr)Al, and intermediate layer of high porosity and a lower layer of α-Fe(Cr,Al). Pores formation took place at the (Fe,Cr)Al - α-Fe(Cr,Al) interface because of the different diffusion coefficients of Al and Fe in the α-Fe(Cr,Al) zone.

Some cracks were initiated at the sample surface. However, due to the high ductility of the scale after the heat treatment these cracks were stopped within the upper part of the scale or within the intermediate zone of high porosity. Crack formation was more frequent on pipe specimens.

It was demonstrated that the described fabrication technology for a Tritium permeation barrier on MANET II steel is relevant for both specimen geometries, flat sheets and pipes, and for inside and outside coatings as well.

Acknowledgement

This work has been performed in the framework of the Nuclear Fusion Project of FZK and was supported by the European Communities within the European Fusion Technology Program.

References

[1] K.S. Forcey, A. Perujo, F. Reiter and P.L. Lolli-Ceroni, J. Nucl. Mater. 200 (1993) 417

[2] A. Perujo, K.S. Forcey and T. Sample, J. Nucl. Mater. 207 (1993) 86

[3] L. Giancarli, L. Baraer, M. Eid, M. Fütterer, E. Proust, X. Raepsaet, J.F. Salavy, L. Sedano, Y. Severi, J. Quintric-Bossy, C. Nardi, L. Petrizzi, Fus. Technol. 26 (1994) 1079

[4] J.D. Fowler, D. Chandra, T.S. Elleman, A.W. Payne and K. Verguese, J. Am. Ceram. Soc. 60 (1977) 155

[5] H. Glasbrenner and H.U. Borgstedt, J. Nucl. Mater. 212-215 (1994) 1561

[6] A. Perujo, T. Sample, E. Serra and H. Kolbe, Fus. Technol. 28 (1995) 1256

[7] G. Benamati, A. Perujo, M. Agostini, A. Serra and N. Antolotti, Proc. 18 th Symp. on Fus. Technol., Karlsruhe, Germany, 1994 (Elsevier Amsterdam, 1995), pp1341

[8] A. Terlain and E. de Vito, Proc. 18 th Symp. on Fus. Technol., Karlsruhe, Germany, 1994 (Elsevier Amsterdam, 1995), pp1337

[9] K.S. Forcey, D.K. Ross and C.H. Wu, J. Nucl. Mater. 182 (1991) 36